SLAC-PUB-7245
SNUTP 95-053
hep-ph/9608247
August 1996

V_{ub} from the Hadron Energy Spectrum in Inclusive Semileptonic B Decays [1]

Christoph Greub[a] **and Soo-Jong Rey**[a,b,c]

Stanford Linear Accelerator Center[a] *& Physics Department*[b]
Stanford University, Stanford, California 94309, USA

Physics Department & Center for Theoretical Physics[c]
Seoul National University, Seoul 151-742 Korea

Abstract

A measurement of the hadron energy spectrum in inclusive semileptonic B decays is proposed as a viable method for extracting $|V_{ub}|$. Compared to the traditional energy spectrum of the charged lepton, the hadron energy spectrum exhibits kinematical advantages such as a wider energy window and a larger signal branching fraction. It is emphasized that the hadron energy spectrum method is most suited for symmetric B factories, such as CLEO. The hadron energy distribution is calculated in the approach of the Altarelli et al. model and of the heavy-quark effective field theory. In both methods, perturbative QCD corrections, the Fermi motion of the b-quark in the B-meson, and the recoil momentum of the B-meson (stemming from the $\Upsilon(4S)$ resonance) are taken into account. We have found excellent agreement between the spectra calculated in both methods, especially in the relevant kinematical region below the charmed meson threshold. The theoretical error to $|V_{ub}|$, which is dominated by the uncertainty of the b-quark mass, is estimated to be at the $\pm 12\%$ level.

Submitted to Physical Review D

[1]Work supported in part by Schweizerischer Nationalfonds and the Department of Energy Contract DE-AC03-76SF00515, U.S.NSF-KOSEF Bilateral Grant, KOSEF Purpose-Oriented Research Grant 94-1400-04-01-3 and SRC-Program, KRF International Coorporation Grant and Nondirected Research Grant 81500-1341, Ministry of Education BSRI Grant 95-2418, and Seoam Foundation Fellowship.

1 Introduction

A precise determination of the Cabibbo-Kobayashi-Maskawa matrix element V_{ub} is an important step for constraining the unitarity triangle. Therefore, it poses a challenge for both theory and experiment [1]. Traditionally, V_{ub} has been extracted from the energy spectrum of the charged lepton in inclusive semileptonic B decays $B \to X_u \ell \nu$ above charm threshold, i.e., for lepton energies E_ℓ above $(m_B^2 - m_D^2)/(2m_B) \approx 2.3$ GeV [2, 3] [2]. As the kinematical endpoint for semileptonic B decays is at $E_\ell = (m_B^2 - m_\pi^2)/(2m_B) \approx 2.6$ GeV, the pure $b \to u\ell^- \overline{\nu}$ transition extends over a relatively narrow window of about 300 MeV, accepting only a fraction of approximately 10 % of the total sample of charmless B decays. Theoretically, the lepton energy spectrum may be calculated from first–principle QCD. Using the tools of the operator product expansion (OPE) and heavy-quark effective field theory [6], one can construct a systematic expansion of the lepton spectrum in powers of Λ/m_b, where Λ is a typical low-energy scale of QCD [7]. However, the relevant lepton energy window from which $|V_{ub}|$ can be extracted lies to a large extent in the so-called endpoint region which extends from the parton model maximum at $E_\ell = m_b/2$ up to the hadronic maximum at $(m_B^2 - m_\pi^2)/(2m_B)$. It is therefore described by genuinely non-perturbative contributions. The difficulty arises from the fact [8] that, close to the partonic endpoint, the expansion parameter is no longer Λ/m_b, but $\Lambda/(2m_b - E_\ell)$. Thus, the theoretical prediction becomes singular when the lepton energy approaches the parton model endpoint; formally, these singularities manifest themselves in delta functions and derivatives of delta functions concentrated at the partonic lepton energy endpoint $m_b/2$. In addition, this region is plagued by large perturbative Sudakov-like double logarithms [9, 10, 11] as well as by small instanton effects [12]. Therefore, in a large part of the lepton energy region in which the extraction of V_{ub} is kinematically possible, a full resummation of Sudakov-like double logarithms [10] and power corrections [13] becomes necessary. In view of the theoretical and experimental difficulties just mentioned, it is desirable to look for other methods.

As an alternative, we propose to extract V_{ub} from the hadron energy spectrum in the inclusive charmless semileptonic B decays $B \to X_u \ell \nu$. Simple kinematical considerations support why this proposal is viable. As the charmed final state threshold is at the D-meson mass, the maximal hadron energy window for charmless semileptonic B decays is given by the range $m_\pi \leq E_{had} \leq m_D$; this window is much wider than the corresponding kinematical window for the lepton energy distribution discussed above, and as we will see later, a much larger fraction of the $B \to X_u \ell \nu$ events becomes accessible, leading to improved statistics. Of course, the theoretical problems addressed in the discussion of the lepton endpoint spectrum are also present in principle in the hadron energy spectrum [14, 15], but to a much lesser extent in the kinematical region relevant for the extraction of V_{ub}. Indeed, up to perturbative QCD corrections, the region around $E_{had} = m_b/2$ is also fully dominated by non-perturbative effects, quite in analogy to the lepton energy endpoint region. Fortunately, this region is well above the charmed hadron final state threshold lying outside the region we are interested in. At the lower end of the hadron energy, $E_{had} \approx 0$, the hadronic mass ranges over a narrow window $0 \leq m_{had}^2 \leq E_{had}^2$, hence, the OPE breaks down again. This region can be avoided by applying a lower cut to the hadron energy; we choose the value 1 GeV. This relatively high lower–cut has

[2] We will discuss the impact on the determination of $|V_{ub}|$ from the recent CLEO measurements of the corresponding exclusive channels $B \to (\pi, \rho, \omega)\, \ell \nu$ [4, 5] later.

the advantage that a wide range of invariant hadronic masses contributes to the hadron energy spectrum; quark-hadron duality, which we implicitly assume in our treatment for the inclusive $B \to X_u \ell \nu$ decay, is then expected to work well. Even after this cut at 1 GeV is made, we are still left with an ample hadron energy window ranging from 1 GeV to m_D. These features in principle make investigations with hadron energy spectra more reliable than with lepton energy spectra.

Experimentally, the hadron energy spectrum in semileptonic B decays may be measured schematically as follows: Working at the $\Upsilon(4S)$ resonance, which decays into $B\bar{B}$, one requires one of the B-mesons to decay semileptonically and the other one hadronically. In the case of a symmetric B-factory, like CLEO, the energy of the hadrons stemming from the semileptonically decaying B-meson can be obtained by measuring the total energy of all the hadrons in the final state and then subtracting $m_{\Upsilon(4S)}/2$. In case of asymmetric B factories, the hadron energy spectrum is harder to measure. One way is to reconstruct in a first step the whole $\Upsilon(4S)$ decay in its rest frame and then perform the analysis just described for the symmetric case. To perform the corresponding boost, one has to measure precisely both the energy and the momentum of each final state hadron, which requires accurate particle identification.

The remainder of this paper is organized as follows. In section 2 the calculation of the hadron energy spectrum is presented. We utilize two methods to account for the bound-state effects. The first one, discussed in section 2.1, uses the Altarelli et al. (ACCMM) model [10] of the B-meson and the second one, presented in 2.2, is based on the heavy-quark effective field theory (HQET) [8]. In both treatments, the perturbative $O(\alpha_s)$ corrections are taken into account. In section 3 the extraction of $|V_{ub}|$ and its theoretical errors are discussed. Finally, in section 4 we give a brief summary together with some comments on the experimental possibilites.

2 Hadron Energy Spectrum

In this section we present the calculation of the hadron energy spectrum which is observed in the rest frame of the $\Upsilon(4S)$ resonance. This frame coincides with the laboratory frame in the case of a symmetric B-factory. We take into account perturbative QCD corrections to $O(\alpha_s)$, but resum Sudakov-like double logarithms. Bound-state effects are evaluated within the ACCMM model [10] and the HQET [8] approaches. We anticipate that both methods will lead to similar results which, for the present case of a heavy to light transition, depend effectively only on one parameter, viz. b-quark mass. Theoretical accounts as to why the two distinct descriptions of bound-state effects in heavy to light transitions should agree, have been given in Ref. [16].

2.1 Hadron Energy Spectrum in the ACCMM Approach

In the ACCMM model the $\bar{B}$-meson consists of a b-quark and a spectator antiquark $\bar{q}$, flying back-to-back in the $\bar{B}$-rest frame with 3-momentum vectors $\vec{p}$ and $-\vec{p}$, respectively; the momentum distribution $\Phi(p)$ of the spectator is assumed to be of Gaussian form

$$\Phi(p) = \frac{4}{\sqrt{\pi} p_F^3} \exp\left(-\frac{p^2}{p_F^2}\right) \quad ; \quad p = |\vec{p}| \quad , \tag{1}$$

normalized according to

$$\int_0^\infty dp\, p^2\, \Phi(p) = 1 \quad . \tag{2}$$

The basic feature of this model is the requirement that in the $\bar{B}$ rest frame the energies of the two constituents have to add up to the $\bar{B}$-meson mass m_B. This is possible only when at least one of the masses of the constituents is allowed to be 3-momentum dependent. Usually, the mass of the spectator m_{sp} is considered to be fixed to a constituent quark mass value, while the b-quark mass becomes momentum dependent,

$$m_b(p)^2 = m_B^2 + m_{sp}^2 - 2m_B\sqrt{p^2 + m_{sp}^2} \quad . \tag{3}$$

We now consider the semileptonic decay $\bar{B} = (b, \overline{q}) \to u(+g)\ell\overline{\nu} + \overline{q}$. The symbols p_b, p_u, p_g, p_ℓ, $p_{\overline{\nu}}$, p_q, p_B, and p_H denote the four-momenta of the b-quark, the u-quark, the gluon, the charged lepton, the anti-neutrino, the spectator, the B-meson, and the hadronic matter of the final state, respectively. In addition, we define the four vector q^μ

$$q = p_\ell + p_{\overline{\nu}} \quad . \tag{4}$$

Due to the fact that $p_b^\mu + p_q^\mu = p_B^\mu$ in the ACCMM model, the vector q^μ is the same with or without the spectator four-momentum, viz.,

$$q = p_B - p_H = p_b + p_q - p_u(-p_g) - p_q = p_b - p_u(-p_g) \quad . \tag{5}$$

For this reason, it is technically easier to concentrate first on the double differential distribution $d^2\Gamma/dq^2dq^0$, because the spectator does not appear explicitly. To achieve this, we first derive the double differential decay rate (including the $O(\alpha_s)$ radiative corrections) for $b \to u(+g)\ell\overline{\nu}$, where the b-quark decays at rest. For simplicity, the u-quark is assumed to be massless. The kinematical variables q^2 and q^0 vary in the region

$$\begin{gathered} 0 \le q^2 \le m_b^2 \quad , \\ \left(q^2\right)^{1/2} \le q^0 \le \frac{m_b^2 + q^2}{2m_b} \quad . \end{gathered} \tag{6}$$

For each q^2, the tree-level process (as well as the virtual gluon corrections) are concentrated at the upper endpoint of the q^0 range in Eq.(6). In the following it is more convenient to introduce dimensionless variables x and y which vary independently in the range $[0, 1]$:

$$\begin{gathered} q^2 = x^2 m_b^2, \\ q^0 = [x + \frac{1}{2}(1-x)^2 y] m_b. \end{gathered} \tag{7}$$

With the above change of variables, we now proceed to calculate the double differential distribution $d^2\Gamma/dxdy$. In terms of the new variables (x, y), the tree-level contribution and the virtual corrections are concentrated at $y = 1$, while the bremsstrahlung corrections give rise to a continuous distribution in the whole (x, y) domain. Individually, both the virtual corrections and bremsstrahlung contributions suffer from infrared and collinear divergences, which occur at $y=1$ for a given value of x. However, if the variable y is integrated over a range $s_0 \leq y \leq 1$ ($s_0 < 1$), these singularities cancel, such that the quantity

$$\frac{d\Gamma}{dx}(s_0) = \int_{s_0}^{1} \frac{d^2\Gamma}{dxdy}dy = \int_{0}^{1} \frac{d^2\Gamma}{dxdy}dy - \int_{0}^{s_0} \frac{d^2\Gamma_{brems}}{dxdy}dy \tag{8}$$

remains finite. The first term on the right hand side (RHS) in Eq.(8) has been calculated in Ref. [17]; the result is

$$\frac{d\Gamma}{dx} \equiv \int_{0}^{1} \frac{d^2\Gamma}{dxdy}dy = 4x(1-x^2)^2(1+2x^2)\,[1-\frac{2\alpha_s}{3\pi}G(x)]\,\Gamma_0 \quad , \tag{9}$$

where Γ_0 and the function $G(x)$ which containes the radiative corrections are given by

$$\Gamma_0 = \frac{G_F^2\, m_b^5\, |V_{ub}|^2}{192\pi^3} \quad , \tag{10}$$

$$G(x) = \frac{[8x^2(1-x^2-2x^4)\log x + 2(1-x^2)^2(5+4x^2)\log(1-x^2) - (1-x^2)(5+9x^2-6x^4)]}{2(1-x^2)^2(1+2x^2)} + \pi^2 + 2\mathrm{Li}(x^2) - 2\mathrm{Li}(1-x^2) \quad . \tag{11}$$

Here $\mathrm{Li}(x)$ is the Spence function defined as

$$\mathrm{Li}(x) = -\int_0^x \frac{dt}{t}\log(1-t). \tag{12}$$

Because the tree-level contribution and virtual corrections are concentrated at $y=1$, the second term on the RHS of Eq. (8) contains the gluon bremsstrahlung contribution only (as indicated by the notation). As the endpoint region is cut off by $s_0 < 1$, this term is finite; consequently, the infrared and collinear regularization is not necessary from the very beginning. We have calculated this term; the result is

$$\int_0^{s_0} \frac{d^2\Gamma_{brems}}{dxdy}dy = 4x(1-x^2)^2(1+2x^2)\,\frac{2\alpha_s}{3\pi}\left(\log^2(1-s_0) + H(s_0)\right)\Gamma_0 \quad , \tag{13}$$

where

$$\begin{aligned} H(s_0) = \quad & \int_0^{s_0} dy \Big(\frac{4}{1-y}\log\frac{2-y(1-x)+\kappa}{2} \\ & - \frac{(1-x)(3+x+xy-y)}{(1+x)^2}\Big[\log(1-y) - 2\log\frac{2-y(1-x)+\kappa}{2}\Big] \\ & - \frac{\kappa}{2(1+x)^2(1+2x^2)}\Big[\frac{7(1+x)(1+2x^2)}{1-y} + (1-x)(3-2x^2)\Big]\Big). \end{aligned} \tag{14}$$

The quantity κ in Eq. (14) is defined as $\kappa = \sqrt{y^2(1-x)^2 + 4xy}$. Combining the two contributions, Eqs.(9) and (13), we obtain

$$\frac{1}{\Gamma_0}\frac{d\Gamma}{dx}(s_0) = 4x(1-x^2)^2(1+2x^2)\left[1 - \frac{2\alpha_s}{3\pi}\log^2(1-s_0) - \frac{2\alpha_s}{3\pi}\left(G(x)+H(s_0)\right)\right]\Theta(1-s_0). \tag{15}$$

The double logarithms arise from the soft and collinear gluons and become important as $s_0 \to 1$. Resumming these double logarithmic terms to all orders, we get

$$\frac{1}{\Gamma_0}\frac{d\Gamma}{dx}(s_0) = 4x(1-x^2)^2(1+2x^2)\,\exp\left(-\frac{2\alpha_s}{3\pi}\log^2(1-s_0)\right)\,\left[1-\frac{2\alpha_s}{3\pi}\left(G(x)+H(s_0)\right)\right]\,\Theta(1-s_0). \tag{16}$$

This expression enables us to reproduce the Sudakov exponentiated double-differential decay rate by differentiating with respect to s_0.

$$\begin{aligned}\frac{1}{\Gamma_0}\frac{d^2\Gamma}{dxdy} &= -\frac{d}{ds_0}\Big(\frac{1}{\Gamma_0}\frac{d\Gamma}{dx}(s_0)\Big)_{s_0=y} = \\ & -4x(1-x^2)^2(1+2x^2)\,\exp\Big(-\frac{2\alpha_s}{3\pi}\log^2(1-y)\Big) \\ &\times \left\{\frac{4\alpha_s}{3\pi}\frac{\log(1-y)}{(1-y)}\Big[1-\frac{2\alpha_s}{3\pi}(G(x)+H(y))\Big]-\frac{2\alpha_s}{3\pi}\frac{dH}{dy}(y)\right\}.\end{aligned} \tag{17}$$

To get the parton level hadron energy spectrum for a b quark decaying at rest, we first re-express Eq.(17) in terms of the variables (q^2, q^0) and then integrate over q^2; this leads to the distribution $d\Gamma/dq^0$. As the hadronic energy E_{had} is related to q^0 by $E_{had} = m_b - q^0$, the spectrum $d\Gamma/dE_{had}$ for a b–quark decaying at rest is readily obtained. To get rid of the b–quark mass dependence m_b^5 in the decay width (as seen e.g. in Eq.(10)) and errors thereof, we present in the following the differential branching ratio dBR/dE_{had} that is obtained by dividing $d\Gamma/dE_{had}$ by the theoretical semileptonic b–quark decay width Γ_{sl} and multiplying this ratio by the experimentally measured semileptonic branching ratio $BR_{sl} = (10.4 \pm 0.4)\%$ [18]:

$$\frac{dBR(B\to X_u\ell\nu)}{dE_{had}} = \left(\frac{1}{\Gamma_{sl}}\frac{d\Gamma}{dE_{had}}\right)\,BR_{sl}. \tag{18}$$

The semileptonic decay width, neglecting the small $B \to X_u\ell\nu$ contribution, reads

$$\Gamma_{sl} = \frac{G_F^2\,m_b^5\,|V_{cb}|^2}{192\pi^3}\,g(m_c/m_b)\,\left(1-\frac{2\alpha_s(m_b)}{3\pi}f(m_c/m_b)\right), \tag{19}$$

where the phase space function $g(u)$ is defined as

$$g(u) = 1 - 8u^2 + 8u^6 - u^8 - 24u^4\log u \quad , \tag{20}$$

and the radiative correction function in an approximate analytic form is given by [11]:

$$f(u) = \left(\pi^2 - \frac{31}{4}\right)\,(1-u)^2 + \frac{3}{2}. \tag{21}$$

The result (based on the the Sudakov improved differential branching ratio as just derived) is shown by the dash-dotted line in Fig. 1 (using $m_b = 4.85$ GeV and $m_c = 1.45$ GeV). To emphasize the effects of the Sudakov resummation, we have also plotted the result obtained in pure $O(\alpha_s)$ perturbation theory [19], i.e., without exponentiation (short-dashed line). This curve exhibits a (integrable) double logarithmic divergence when $E_{had} = m_b/2$ is approached from above. The effects of the exponentiation are therefore most prominent in the region around $m_b/2$ as illustrated in Fig. 1, because Sudakov-exponentiation suppresses the singularity just mentioned. We stress, however, that the effect of exponentiation is negligibly small in the whole region below the charmed hadron threshold we are mostly interested in. This should be contrasted with the case of the energy spectrum of the charged lepton near the kinematical endpoint where these effect are most pronounced.

Another interesting aspect concerning the radiative corrections to the hadron energy spectrum is that the kinematical boundary of the hadron energy depends on whether the final state contains bremsstrahlung gluons or not. In the absence of bremsstrahlung gluons, the kinematical endpoint is at $m_b/2 = 2.425$ GeV as can be seen form the long-dahed curve representing the result without QCD corrections. Fig. 1 clearly illustrates that, above $E_{had} = 2.425$ GeV, a significant tail due to gluon bremsstrahlung, hence of order $\alpha_s(m_b)$ in strength, is present in the spectrum.

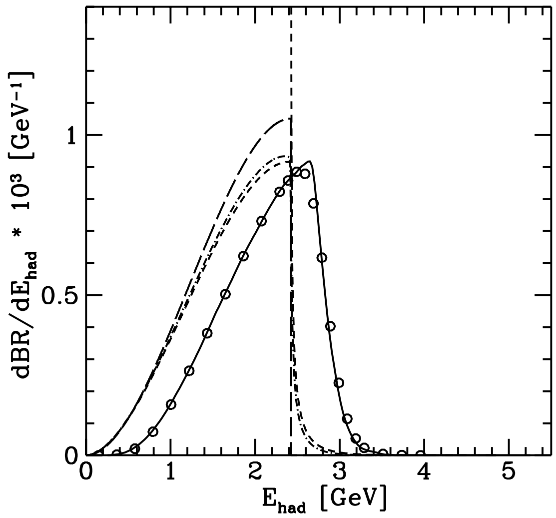

Figure 1: The long-dashed line shows the hadron energy spectrum for a b-quark decaying at rest without taking into account any QCD corrections. The short-dashed line is the corresponding spectrum including $O(\alpha_s)$ virtual and bremsstrahlung corrections. The result after exponentiating the Sudakov double logarithms (discussed in the present section) is shown by the dash-dotted line. The solid line shows the hadron energy spectrum for a B-meson decaying at rest. The bound state effects are calculated with the ACCMM model with $p_F = 344$ MeV and $m_{sp} = 150$ MeV (corresponding to $\langle m_b \rangle = 4.85$ GeV). The open circles show the hadron energy spectrum due to a B-meson decaying at flight with a momentum $|p_B| = 330$ MeV.

We now turn to implement the bound–state effects using the ACCMM model. We start from the double differential distribution $d\Gamma/dq^2dq^0$ in Eq. (17). As the b-quark moves with momentum $\vec{p}$ inside the B-meson, we first replace the mass m_b by $m_b(p)$ as given in Eq. (3). We then Lorentz boost the double differential distribution and get the spectrum for a b-quark decaying at flight (momentum $\vec{p}$). Finally we convolute the spectrum with the ACCMM distribution function given in Eq. (1). This leads to the ACCMM averaged quantity $d\Gamma/dq^2dq^0$ for a B-meson decaying at rest. Again, this distribution is straightforwardly converted to $d\Gamma/dE_{had}$. To get the differential branching ratio, we replace the b–quark mass m_b in the expression for the semileptonic decay width in Eq. (19) by the ACCMM average value $\langle m_b\rangle$ derived by applying the ACCMM convolution to the total semileptonic decay rate. This ACCMM averaged b-quark mass is given by

$$\langle m_b^5\rangle = \int dp\, p^2\, (m_b(p))^5\, \Phi(p) \quad . \tag{22}$$

The $m_b - m_c$ mass difference is reliably calculated to be 3.40 GeV by HQET [20]. Therefore, we set $m_c = \langle m_b\rangle - 3.40\,\mathrm{GeV}$ in the Γ_{sl}. The result is shown in Fig. 1 by the solid line; here we have used $p_F = 344$ MeV and $m_{sp} = 150$ MeV, which yields $\langle m_b\rangle = 4.85$ GeV according to Eq. (22). As shown in Fig. 1, the main effect of the Fermi motion of the b-quark inside B-meson is to shift the perturbative hadron energy spectrum uniformly to higher energies by about 300 MeV. We will elaborate this point in more detail when discussing the HQET approach to the bound-state effects, where the same result can be understood in a more transparent way.

There is one more source of Doppler shift to the hadron energy spectrum. At a symmetric B-factory the B-meson is produced from the decay of the $\Upsilon(4S)$ resonance. Due to the released binding energy the B-mesons are produced with a momentum $|\vec{p}_B| \approx 330$ MeV in the $\Upsilon(4S)$ rest frame. We have also worked out this effect to the spectrum; the corresponding result is shown in Fig. 1 by open circles. As this effect is very small, we will not consider it any more in foregoing discussions.

Although the ACCMM model has two input parameters, viz. p_F and m_{sp}, it turns out that the hadron energy spectrum is sensitive only to one parameter, namely, the average b–quark mass $\langle m_b\rangle$, which is a function of p_F and m_{sp} (see Eq. (22)) [3]. To illustrate this point, we have chosen two different pairs of (p_F, m_{sp}) values, which both correspond to the same value of $\langle m_b\rangle$ (=4.85 GeV in the present case). The correspondig result plotted in Fig. 2 indicates little dependence on p_F and m_{sp}, once $\langle m_b\rangle$ is hold fixed. In Fig. 3, we have varied $\langle m_b\rangle$ over the range indicated in the plot. We have found that the hadron energy spectrum depends on $\langle m_b\rangle$ rather strongly, especially in the region below the charmed hadron threshold.

2.2 Hadron Energy Spectrum in the HQET Approach

Next we calculate the hadron energy spectrum using the HQET approach. Since the derivation is discussed in detail in [15], we only repeat the results relevant for our discussions. In the following we take into account the leading corrections in α_s and $1/m_b$, but we neglect mixed higher–order corrections of the order $\alpha_s \frac{1}{m_b}$. We assign the b quark the same four velocity v^μ as the heavy meson and define the dimensionless parton level quantity $\hat{E}_0$ as

$$\hat{E}_0 = \frac{v\cdot(p_b - q)}{m_b} = 1 - \frac{q\cdot v}{m_b} \quad . \tag{23}$$

The physical hadron energy E_{had} is given as

$$E_{had} = v\cdot(P_B - q) = m_B - q\cdot v \quad . \tag{24}$$

The leading order equality between $m_B\hat{E}_0$ and E_{had} gets modified by corrections linear in $1/m_b$

$$E_{had} = \bar{\Lambda} - \frac{\lambda_1 + 3\lambda_2}{2m_B} + \left(m_B - \bar{\Lambda} + \frac{\lambda_1 + 3\lambda_2}{2m_B}\right)\hat{E}_0 + \cdots \quad , \tag{25}$$

[3] It has been pointed out that transitions from heavy quarks to light quarks with masses $m_q \le (\bar{\Lambda} m_b)^{1/2}$ always give rise effectively to a one-parameter dependence [16].

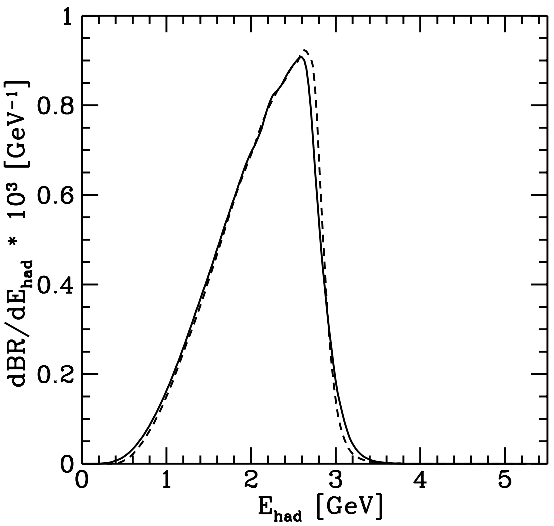

Figure 2: The hadron energy spectrum (based on the ACCMM model) is shown for two different pairs of model paramters (p_F, m_{sp}). The solid line corresponds to $(374\text{ MeV}, 0)$ while the dashed line represents the result for $(252\text{ MeV}, 300\,\text{MeV})$. Both set correspond to the same value of the b-quark mass $\langle m_b \rangle = 4.85$ GeV.

where we have used the relationship

$$m_B = m_b + \bar{\Lambda} - \frac{\lambda_1 + 3\lambda_2}{2m_b} + \cdots \tag{26}$$

between the b quark and the B-meson masses. The ellipses in Eqs. (25) and (26) stand for higher order corrections in the $1/m_b$ expansion. We split the differential spectrum $\frac{d\Gamma}{d\hat{E}_0}$ into two parts:

$$\frac{d\Gamma}{d\hat{E}_0} = \frac{d\Gamma^{1/m_b^2}}{d\hat{E}_0} + \frac{d\Gamma^{\alpha_s}}{d\hat{E}_0} \quad . \tag{27}$$

The first term on the right hand side (RHS) of Eq. (27) consists of the $1/m_b^2$ corrections and has been calculated in [15]. For $m_u = 0$ one gets $(0 \leq \hat{E}_0 \leq 1/2)$

$$\begin{aligned} \frac{1}{\Gamma_0}\frac{d\Gamma^{1/m_b^2}}{d\hat{E}_0} &= 16\,\hat{E}_0^2\,[3 - 4\hat{E}_0] \\ &+ 16\left[\frac{\lambda_1}{2m_B^2}\left(-6\hat{E}_0 + 12\hat{E}_0^2 + \frac{20}{3}\,\hat{E}_0^3\right) + \frac{\lambda_2}{2m_B^2}\left(-3 - 6\hat{E}_0 + 36\hat{E}_0^2 + 20\hat{E}_0^3\right)\right] \\ &+ \left(\frac{5\lambda_1}{3m_B^2} - \frac{\lambda_2}{m_B^2}\right)\delta(\hat{E}_0 - 1/2) + \frac{\lambda_1}{6m_B^2}\,\delta'(\hat{E}_0 - 1/2) + O(\alpha_s; 1/m_b^3) \quad , \end{aligned} \tag{28}$$

with Γ_0 given in Eq. (10). The second term on the RHS of Eq. (27) contains the perturbative $O(\alpha_s)$ corrections; it has been calculated by Czarnecki et al. [19]. For completeness, we list their result for a massless u-quark:

$$\frac{1}{\Gamma_0}\frac{d\Gamma^{\alpha_s}}{d\hat{E}_0} = \frac{32\alpha_s}{3\pi}\,\mathcal{G}_1(\hat{E}_0) \quad , \tag{29}$$

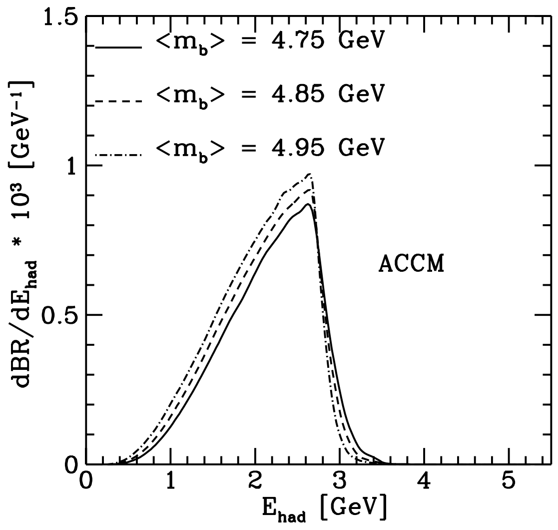

Figure 3: The hadron energy spectrum based on the ACCMM approach is shown for different values of the b-quark mass $\langle m_b \rangle$.

where the function $\mathcal{G}_1$ for $0 \leq \hat{E}_0 \leq 1/2$ reads

$$\begin{aligned}\mathcal{G}_1(\hat{E}_0) &= \hat{E}_0^2 \left\{ \frac{1}{90} \left(16\hat{E}_0^4 - 84\hat{E}_0^3 + 585\hat{E}_0^2 - 1860\hat{E}_0 + 1215\right) \right. \\ &\left. +(8\hat{E}_0 - 9)\, \log 2\hat{E}_0 + 2(4\hat{E}_0 - 3) \left[\frac{\pi^2}{2} + \mathrm{Li}(1 - 2\hat{E}_0)\right] \right\} \quad , \qquad (30)\end{aligned}$$

while for $1/2 < \hat{E}_0 \leq 1$

$$\begin{aligned}\mathcal{G}_1(\hat{E}_0) &= \frac{1}{180}(1 - \hat{E}_0) \left(32\hat{E}_0^5 - 136\hat{E}_0^4 + 1034\hat{E}_0^3 - 2946\hat{E}_0^2 + 1899\hat{E}_0 + 312\right) \\ &- \frac{1}{24}\, \log(2\hat{E}_0 - 1) \left(64\hat{E}_0^3 - 48\hat{E}_0^2 - 24\hat{E}_0 - 5\right) \\ &+ \hat{E}_0^2\,(3 - 4\hat{E}_0) \left[\frac{\pi^2}{3} - 4\mathrm{Li}(1/(2\hat{E}_0)) + \log^2(2\hat{E}_0 - 1) - 2\log^2(2\hat{E}_0)\right] \quad . \qquad (31)\end{aligned}$$

Using relation (25) between $\hat{E}_0$ and E_{had}, the corresponding hadron energy spectrum $\frac{1}{\Gamma_0}\frac{d\Gamma}{dE_{had}}$ is readily obtained. While the quantity $\frac{1}{\Gamma_0}\frac{d\Gamma}{d\hat{E}_0}$ is free from corrections linear in $1/m_b$, there are such corrections in the hadron energy spectrum $\frac{1}{\Gamma_0}\frac{d\Gamma}{dE_{had}}$. The differential branching ratio in the HQET approach is then given by

$$\frac{dBR(B \to X_u e\nu)}{dE_{had}} = \frac{|V_{ub}|^2}{|V_{cb}|^2} \frac{\left(\frac{1}{\Gamma_0}\frac{d\Gamma}{dE_{had}}\right)}{g(m_c/m_b)} BR_{sl} \left[1 - \frac{2\alpha_s(m_b)}{3\pi} f(m_c/m_b) + \frac{h(m_c/m_b)}{2m_b^2}\right]^{-1} \quad , \quad (32)$$

where the phase space function $g(u)$ and the radiative correction function $f(u)$ are listed in Eqs. (20) and (21), respectively. The function $h(u)$ contains the $1/m_b^2$ corrections to the semileptonic decay $B \to X_c \ell \nu$; it reads

$$h(u) = \lambda_1 + \frac{\lambda_2}{g(u)} \left[-9 + 24u^2 - 72u^4 + 72u^6 - 15u^8 - 72u^4 \log u \right] \quad . \tag{33}$$

To illustrate the qualitative features of the non-perturbative corrections, it is instructive to retain only the dominant terms which are linear in $1/m_b$. The relation between E_{had} and $\hat{E}_0$ (given in Eq. (25)) then simplifies to $E_{had} = \bar{\Lambda} + m_b \hat{E}_0 = \bar{\Lambda} + E_0$, where E_0 is the hadron energy at the parton level. Therefore, the dominant bound–state effect is simply a uniform shift of the parton level hadron energy spectrum to higher energies by an amount of $\bar{\Lambda}$; exactly the same feature was also noted when implementing the bound state effects using the ACCMM approach (see Fig. 1). From these considerations it is clear that the most important parameter is $\bar{\Lambda} \approx m_B - m_b$, while the parameters λ_1 and λ_2 play a relatively minor role. In the numerical evaluations we therefore have used the fixed values $\lambda_1 = -0.5\,\text{GeV}^2$ and $\lambda_2 = 0.12\,\text{GeV}^2$ and presented the results as a function of m_b (or, equivalently, $\bar{\Lambda}$) only.

In Fig. 4 we compare the ACCMM and the HQET approaches. As an example we have chosen $m_b = \langle m_b \rangle = 4.85$ GeV. The plot illustrates that the two methods agree with each other rather well, especially in the energy range 1 GeV $\leq E_{had} \leq m_D$. We have checked that this agreement holds everywhere in the relevant b quark mass range $m_b = (4.8 \pm 0.2)$ GeV.

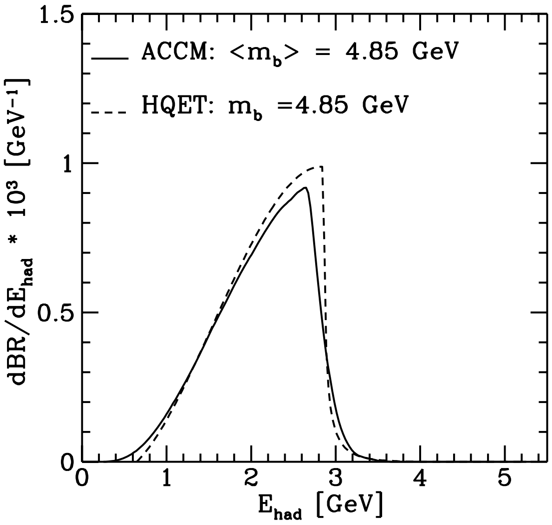

Figure 4: The hadron energy spectrum is shown for two different descriptions of the bound state effects. The solid curve shows the result obtained by using the ACCMM model while the dashed line shows the HQET result.

3 Extraction of V_{ub} from the Hadron Energy Spectrum

As discussed in the Introduction, theoretical predictions for the hadron energy spectrum are expected to be rather reliable in the relevant kinematical region below the D-meson mass, once a sufficiently high lower–cut in the hadron energy is made at the same time. Choosing the lower cut at 1 GeV, the invariant hadronic mass ranges from m_π up to $E_{had} \geq 1\,\mathrm{GeV}$ for all values of the hadronic energy in the window $1\,\mathrm{GeV} \leq E_{had} \leq m_D$. In this case a large number of different hadronic final states contributes to the spectrum; hence, quark-hadron duality should hold quite well. We therefore propose to measure experimentally the kinematical branching ratio defined by

$$BR^{kin}(B \to X_u \ell \nu) = \int_{1\,GeV}^{m_D} \frac{dBR(B \to X_u \ell \nu)}{dE_{had}}\, dE_{had} \quad . \tag{34}$$

A comparison with the corresponding theoretical quantity then allows to extract the CKM ratio $|V_{ub}|/|V_{cb}|$. While leaving aside the experimental question how accurately the kinematical branching ratio can be measured now or in the future, we would like to point out in the following that the theoretical uncertainties in this observable are small enough to reduce substantially the present theoretical error on $|V_{ub}|$. As it turns out that the theoretical error of the kinematical branching ratio is dominated by the uncertainty of the effective b quark mass (i.e., m_b in the HQET approach and $\langle m_b \rangle$ in the ACCMM approach), we take into account only this effect in the following analysis [4]. A reasonable range for the value of m_b can be inferred from the measurement of the lepton energy spectrum in the inclusive decays $B \to X_{c,u} \ell \nu$. Fitting to the ACCMM model, CLEO extracted p_F to be 264 ± 16 MeV (using a value of $m_{sp} = 150$ MeV for the mass of the spectator quark) [2, 21]. In a more recent analysis using lepton tags [22], they extracted the value $p_F = 347 \pm 68$ MeV. We thus choose to vary p_F in the somewhat larger range $200\,\mathrm{MeV} \leq p_F \leq 435\,\mathrm{MeV}$ which covers both measurements. Using Eq. (22), this p_F-range translates into the $\langle m_b \rangle$-range

$$4.75\,\mathrm{GeV} \leq \langle m_b \rangle \leq 5\,\mathrm{GeV}. \tag{35}$$

We note that this range is also compatible with the best value ($\langle m_b \rangle$=4.77 GeV) fitted from the photon energy spectrum in $B \to X_s \gamma$ [23].

So far, we have not discussed the question, if the cascade decay $b \to cX \to s \ell \nu X$, where the symbol X denotes light quarks, can fake a $b \to u \ell \nu$ transition. If the c-quark is off-shell, this process can kinematically fake a $b \to u \ell \nu$ transition, but in this case the process is higher order in the weak interaction, hence negligible. On the other hand, if the c quark is on-shell, the energy of the hadronic system X is larger than m_D. Therefore, this cascade process is not a backgound to the $b \to u \ell \nu$ transition; this is in contrast to the endpoint analysis of the lepton energy spectrum, where the cascade process has to be subtracted out.

To get an idea what fraction R of the total semileptonic $b \to u$ events will be captured in the energy window $1\,\mathrm{GeV} \leq E_{had} \leq m_D$, we have used the present central value for $|V_{ub}|/|V_{cb}| = 0.08$ [24]. The m_b dependence of the kinematical branching ratio and of the fraction R are shown in Table 1 for both the ACCMM and the HQET approaches. Varying m_b in the range specified in Eq. (35) and using the results for BR^{kin}_{HQET} in Table 1 (where the variation is somewhat larger than in the ACCMM model), we obtain

$$BR^{kin} = \frac{|V_{ub}|^2}{|V_{cb}|^2} \times (4.51 - 6.61) \times 10^{-2} \quad . \tag{36}$$

[4]The dependence of the kinematical branching ratio on the numerical value of α_s is very small. In our numerical evaluations we have taken $\alpha_s = 0.205$.

m_b (GeV)	$BR^{kin}_{ACCMM} * 10^4$	R_{ACCMM} (%)	$BR^{kin}_{HQET} * 10^4$	$R_{HQET}(\%)$
4.60	2.41	23	2.17	21
4.65	2.58	24	2.40	22
4.70	2.76	25	2.64	24
4.75	2.94	26	2.89	25
4.80	3.15	27	3.14	27
4.85	3.37	28	3.41	28
4.90	3.59	29	3.68	29
4.95	3.83	30	3.95	31
5.00	4.07	31	4.23	32

Table 1: The kinematical branching ratio BR^{kin} defined in Eq. (34) and the corresponding fraction R of the semileptonic $b \to u$ events lying in the energy window $1\,\text{GeV} \leq E_{had} \leq m_D$ are given as a function of m_b for the ACCMM and the HQET approach. $|V_{ub}|/|V_{cb}| = 0.08$ is assumed.

Denoting the measured kinematical branching ratio by BR^{kin}_{exp}, one can extract $|V_{ub}|/|V_{cb}|$ to be

$$\frac{|V_{ub}|}{|V_{cb}|} = \sqrt{BR^{kin}_{exp}} \cdot (4.30 \pm 0.41) \quad . \tag{37}$$

This implies that the theoretical error of the ratio $|V_{ub}|/|V_{cb}|$ is approximately $\pm 10\%$. Taking the somewhat larger range $m_b = (4.80 \pm 0.15)$ GeV adopted in [1, 25], we get from Table 1

$$\frac{|V_{ub}|}{|V_{cb}|} = \sqrt{BR^{kin}_{exp}} \cdot (4.60 \pm 0.56) \quad , \tag{38}$$

which implies a theoretical error of about 12 %.

To illustrate that our proposal has the potential to lead to a more precise determination of V_{ub}, it is instructive to briefly review the present situation. The traditional inclusive lepton endpoint spectrum analysis done at CLEO [2] and at ARGUS [3], leads to the result $|V_{ub}|/|V_{cb}| = 0.08 \pm 0.03$, where the error is dominated by theory [26]. A recent new input to this quantity is provided by the measurements of the exclusive semileptonic decays $B \to (\pi, \rho, \omega)\, \ell\nu$ [4, 5]. The value for $|V_{ub}|$ quoted in the most recent analysis [5] is $|V_{ub}| = (3.3 \pm 0.2^{+0.3}_{-0.4} \pm 0.7) \times 10^{-3}$, where the errors are statistical, systematic and estimated model dependence, after excluding models which are unable to predict the correct π/ρ ratio.

4 Summary and Discussion

In this paper we have proposed to measure the hadron energy spectrum from inclusive semileptonic B decays in order to extract the CKM matrix element V_{ub} with improved precision. The main advantage of our proposal is that the energy window, in which the $b \to c\ell^-\overline{\nu}$ transition is kinematically absent ($E_{had} < m_D$), is much wider than the corresponing window available in the traditional lepton energy endpoint spectrum analysis. Even after imposing a relatively high lower–cut at $E_{had} = 1$ GeV (in order to avoid the region of phase space where the range in the invariant hadronic mass is too narrow to invoke quark-hadron duality), a much larger fraction of the $b \to u\ell^-\overline{\nu}$ events is captured in the remaining window $1\,\mathrm{GeV} \leq E_{had} \leq m_D$ than in the lepton spectrum endpoint analysis.

After calculating the hadron energy spectrum in QCD improved perturbation theory, we have implemented the bound-state effects using both the ACCMM and the HQET approaches; the two methods gave essentially the same result, in particular in the relevant kinematical window. Qualitatively, the dominant bound state effect is a uniform shift of the parton level spectrum. We have pointed out that the theoretical error in the ratio $|V_{ub}|/|V_{cb}|$, which is dominated by the present uncertainties in the m_b quark mass, is about a factor of 2 to 3 smaller than the one in the lepton endpoint spectrum analysis and about a factor of 2 smaller than the model uncertainties in the branching fractions of the exclusive decays $B \to (\pi, \rho, \omega)\,\ell\nu$. Therefore, for both statistical and theoretical reasons, the extraction of $|V_{ub}|$ from the hadron energy spectrum seems very attractive.

On the experimental side, our proposal is most suited for a symmetric B-factory running at the $\Upsilon(4S)$ resonance, which is currently available at the CLEO experiment. Tagging the events from the $\Upsilon(4S)$ decay, in which one B-meson is decaying semileptonically and the other one nonleptonically, the energy of the final state hadrons stemming from the semileptonically decaying B-meson is easily obtained by adding up the energies of all the hadrons in the final state and then subtracting $m_\Upsilon/2$. On the other hand, in asymmetric B factories, the hadron energy spectrum is harder to measure because one first has to reconstruct the corresponding distribution in the rest frame of $\Upsilon(4S)$; to perform the corresponding boost, one has to measure precisely both the energy and the momentum of each final state hadron, which requires accurate particle identification.

The spectrum of the invariant hadronic mass ($d\Gamma/dm_X$) in inclusive semileptonic decays $B \to X_{c,u}\ell\nu$ is another source from which one may try to extract V_{ub}. Requiring m_X to be below m_D, the process $B \to X_c\ell\nu$ can be totally supressed. Consequently, the integral of the hadron invariant mass distribution below m_D is another observable proportional to $|V_{ub}|^2$. As the invariant mass is integrated over a large range, which covers about 95 % of all the $b \to u\ell^-\overline{\nu}$ events [27], this observable is also theoretically viable. However, we believe that the invariant mass spectrum is more difficult to measure than the hadron energy spectrum proposed in this paper, because first, one has to measure the four momenta of all the final state hadrons from the $\Upsilon(4S)$ decay and second, one has to find a subset of final state hadrons with an invariant mass of m_B, corresponing to the B-meson which decays hadronically. Only then the invariant mass of the semileptonically decaying B-meson can be determined.

Finally, we point out a potentially interesting possibility of a direct measurement of $\alpha_s(m_b)$ or $\overline{\Lambda}$. We have shown that, once the real gluon bremsstrahlung correction is taken into account, the kinematic maximum of the hadron energy shifts from the tree–level (and virtual gluon correction) endpoint $(m_b^2 + m_q^2)/2m_b$ to m_b. For the $b \to u$ case, Fig. 1 shows that the bremsstrahlung tail extends approximately 400 MeV beyond $m_b/2$. We also have shown that the dominant bound-state effect is to shift the spectrum by $\overline{\Lambda}$ for both ACCMM and HQET approaches. Therefore, once $\overline{\Lambda}$ is known accurately, then $\alpha_s(m_b)$ can be extracted directly from the bremsstrahlung tail spectrum. Alternatively, given an accurate value of $\alpha_s(m_b)$, the non-perturbative parameter $\overline{\Lambda}$ can be accurately measured. Since the bremsstrahlung spectrum of $b \to c$ extends further out than that of $b \to u$, the above proposal should be most suited for the

$b \to c$ transition. In this case, one has to take into account the finite c-quark mass dependence of the perturbative QCD corrections and bound-state effects.

We thank A. Ali, S.J. Brodsky, B. Grinstein, S.-K. Kim, J.H. Kühn, Y.-J. Kwon, M. Lu, P. Minkowski, R. Poling, E. Thorndike, and R. Wang for helpful discussions.

References

[1] For an up-to-date pedagogical review, see A. Ali, *B Decays, Flavor Mixings and CP Violation in the Standard Model*, DESY-96-106 preprint, hep-ph/9606324 (1996).

[2] J. Bartelt et al. (CLEO Collaboration), *Inclusive Measurement of the B-Meson Semileptonic Branching Fractions*, CLEO Conf. 93-19, Lepton-Photon 1993 at Cornell University.

[3] H. Albrecht et al. (ARGUS Collaboration), preprint DESY 96-015 (1996).

[4] T. Skwarnicki, preprint [hep-ph/9512395], to appear in: Proc. of the 17th Int. Symp. on Lepton Photon Interactions, Beijing, P.R. China, August 1995; E. Thorndike, in: Proc. of the Int. Europhys. Conf. on High Energy Physics, Brussels, Belgium, July 27-31, 1995; R. Ammar et al. (CLEO Collaboration), contributed paper to this conference (EPS-0165) (1995).

[5] J.P. Alexander et al. (CLEO Collaboration), preprint CLEO CONF 96-16, ICHEP96 PA05-081, submitted to Phys. Rev. Lett..

[6] For pedagogical reviews, see, for example, N. Isgur and M.B. Wise, *Heavy Quark Symmetry*, in *Heavy Flavors*, eds. A.J. Buras and M. Lindner, World Scientific Pub. Co. (1992, Singapore); M. Neubert, *Heavy Quark Masses, Mixing Angles and Spin Flavor Symmetry*, Lectures given at TASI '93, hep-ph/9404296 (1993); B. Grinstein, *An Introduction to Heavy Mesons*, Lectures given at 6th Mexican School of Particles and Fields, hep-ph/9508227 (1995).

[7] M. Voloshin and M. Shifman, Sov. J. Nucl. Phys. **41** (1985) 120; J. Chay, H. Georgi and B. Grinstein, Phys. Lett. **B247** (1990) 399; I.I. Bigi, N.G. Uraltsev and A.I. Vainshtein, Phys. Lett. **B293** (1992) 430; I.I. Bigi, M. Shifman, N.G. Uraltsev and A.I. Vainshtein, Phys. Rev. Lett. **71** (1993) 496; B. Blok, L. Koyrakh, M. Shifman and A.I. Vainshtein, Phys. Rev. **D49** (1994) 3356; **50**, 3572(E) (1994);

[8] T. Mannel, Nucl .Phys. **B413** (1994) 396; A.V. Manohar and M.B. Wise, Phys. Rev. **D49** (1994) 1310; M. Neubert, Phys. Rev. **D49** (1994) 3392.

[9] V. Sudakov, Zh. Eksp. Teor. Fiz. **30** (1956) 87 [Sov. Phys. JETP **3** (1956) 65].

[10] G. Altarelli et al., Nucl. Phys. **B208** (1982) 365.

[11] C. Corbo, Nucl. Phys. **B212** (1983) 99; N. Cabibbo, G. Corbo and L. Maiani, Nucl. Phys. **B155** (1979) 93; A. Falk, E. Jenkins, A. Manohar and M.B. Wise, Phys. Rev. **D49** (1994) 4553;M. Luke, M. Savage and M.B. Wise, Phys. Lett. **B343** (1995) 329; R. Akhoury and I.Z. Rothstein, Phys. Rev. **D54** (1996) 2349.

[12] J. Chay and S.-J. Rey, Zeit. für Phys. **C68** (1995) 431; ibid. 425; A. Falk, A. Kyatkin, Phys.Rev. **D52** (1995) 5049.

[13] I.I. Bigi, M.A. Shifman, N.G. Uraltsev and A.I. Vainshtein, Int.J.Mod.Phys. **A9** (1994) 2467-2504; T. Mannel and M. Neubert, Phys. Rev. **D50** (1994) 2037.

[14] A.O. Bouzas and D. Zappalà, Phys. Lett. **B333** (1994) 215.

[15] A. Falk, M. Luke and M. Savage, Phys. Rev. **D53** (1996) 2491.

[16] I.I. Bigi, N.G. Uraltsev and A.I. Vainshtein, Phys. Lett. **B293** (1992) 430; C. Csaki and L. Randall, Phys. Lett. **B324** (1994) 451.

[17] M. Ježabek and J.H. Kühn, Nucl. Phys. **B314** (1989) 1.

[18] L. Gibbons (CLEO Collaboration), in Proceedings of the XXX Rencontres de Moriond, Les Arcs, March 1994.

[19] A. Czarnecki, M. Ježabek and J.H. Kühn, Acta. Phys. Pol. **B20** (1989) 961; Nucl. Phys. **B320** (1989) 20.

[20] M. Shifman, N.G. Uraltsev and A. Vainshtein, Phys. Rev. **D51** (1995) 2217; M.B. Voloshin, Phys. Rev. **D51** (1995) 4934.

[21] R. Poling (CLEO Collaboration), private communication.

[22] M. Barish et al. (CLEO Collaboration), Phys. Rev. Lett. **76** (1996) 1570.

[23] A. Ali and C. Greub, Phys. Lett. **B361** (1995) 146.

[24] L. Montanet et al. (Particle Data Group), Phys. Rev. **D50** (1994) 1173.

[25] E. Bagan et al., Phys. Lett. **B278** (1992) 457; M. Neubert, Phys. Rep. **B245** (1994) 259.

[26] P. Ball, V.M. Braun and H.G. Dosch, Phys. Rev. **D48** (1993) 2110.

[27] J. Dai, Phys. Lett. **B333** (1994) 212; V. Barger and C.S. Kim, Phys. Lett. **B251** (1990) 629.